Electronic Supplementary Material (ESI) for Journal of Materials Chemistry A.

Host dependent electrocatalytic hydrogen evolution of Ni/TiO_2 composite

Peng Zhou,[a] Shuhua Wang,[b] Guangyao Zhai,[a] Xingshuai Lv,[b] Yuanyuan Liu,*[a] Zeyan Wang,[a] Peng Wang,[a] Zhaoke Zheng,[a] Hefeng Cheng,[a] Ying Dai,[b] and Baibiao Huang*[a]

[a]State Key Laboratory of Crystal Materials, Shandong University, Jinan 250100, China.

[b]School of Physics, Shandong University, Jinan 250100, China.

† *Email: yyliu@sdu.edu.cn; *Email: bbhuang@sdu.edu.cn

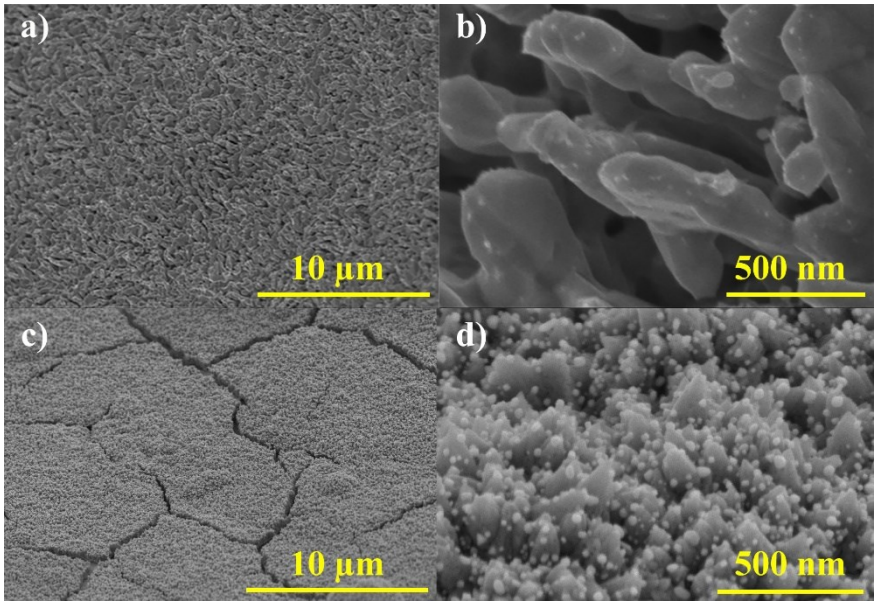

Figure S1. The SEM images of Ni (a, b) and Ni/TiO_2-form-A-S (c, d) samples.

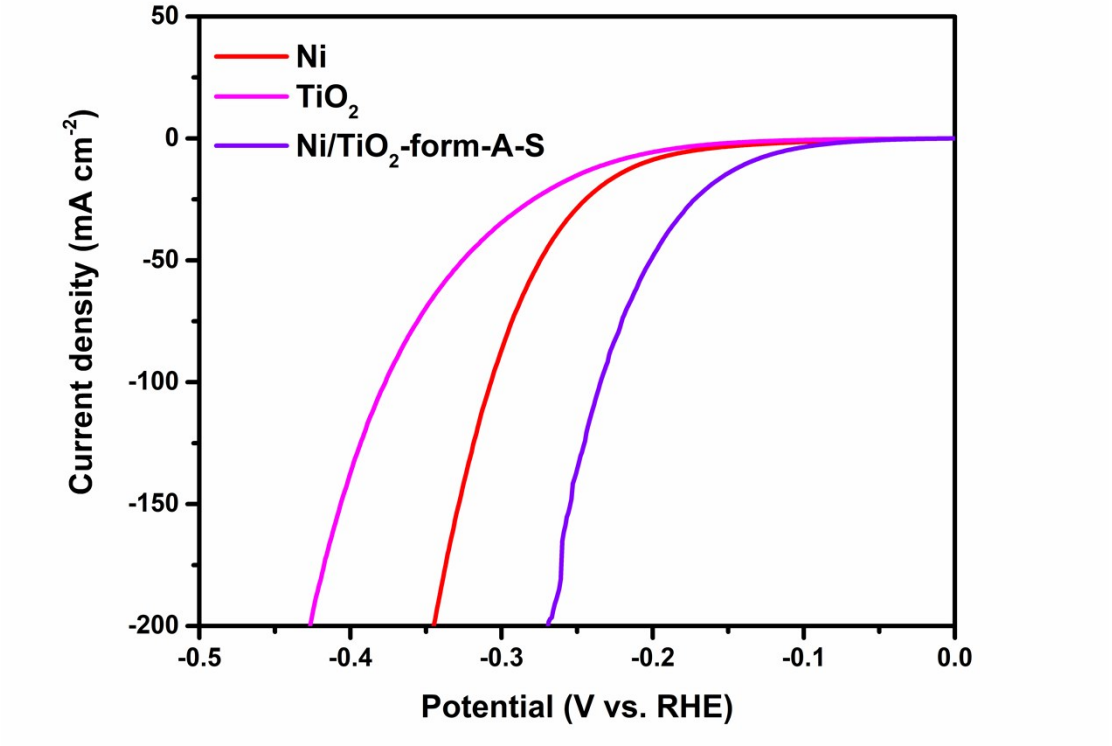

Figure S2. The LSV curves of Ni, Ni/TiO_2-form-A-S and TiO_2 samples.

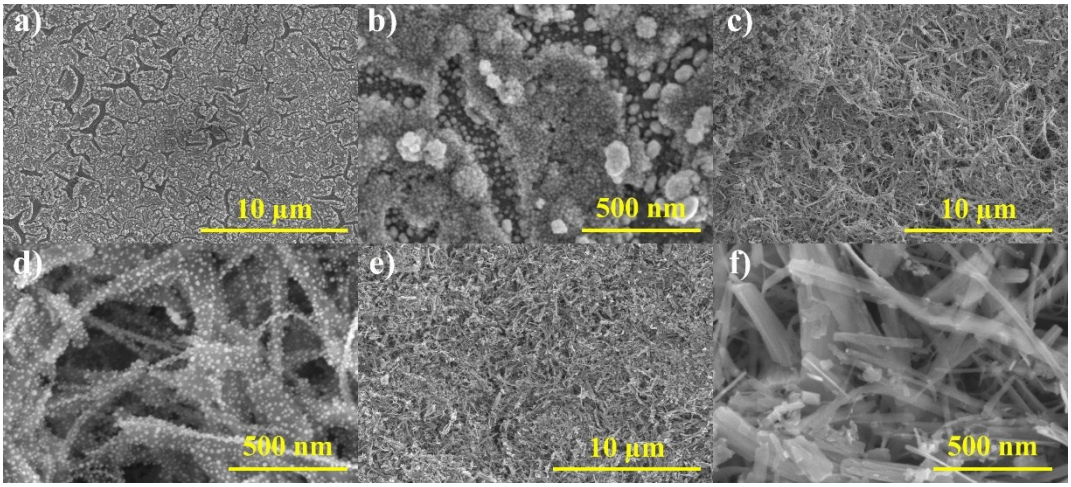

Figure S3. The SEM images of Ni-Ti foil (a, b), Ni/TiO_2-form-B-S (c, d) and TiO_2-Ti foil (e, f) samples.

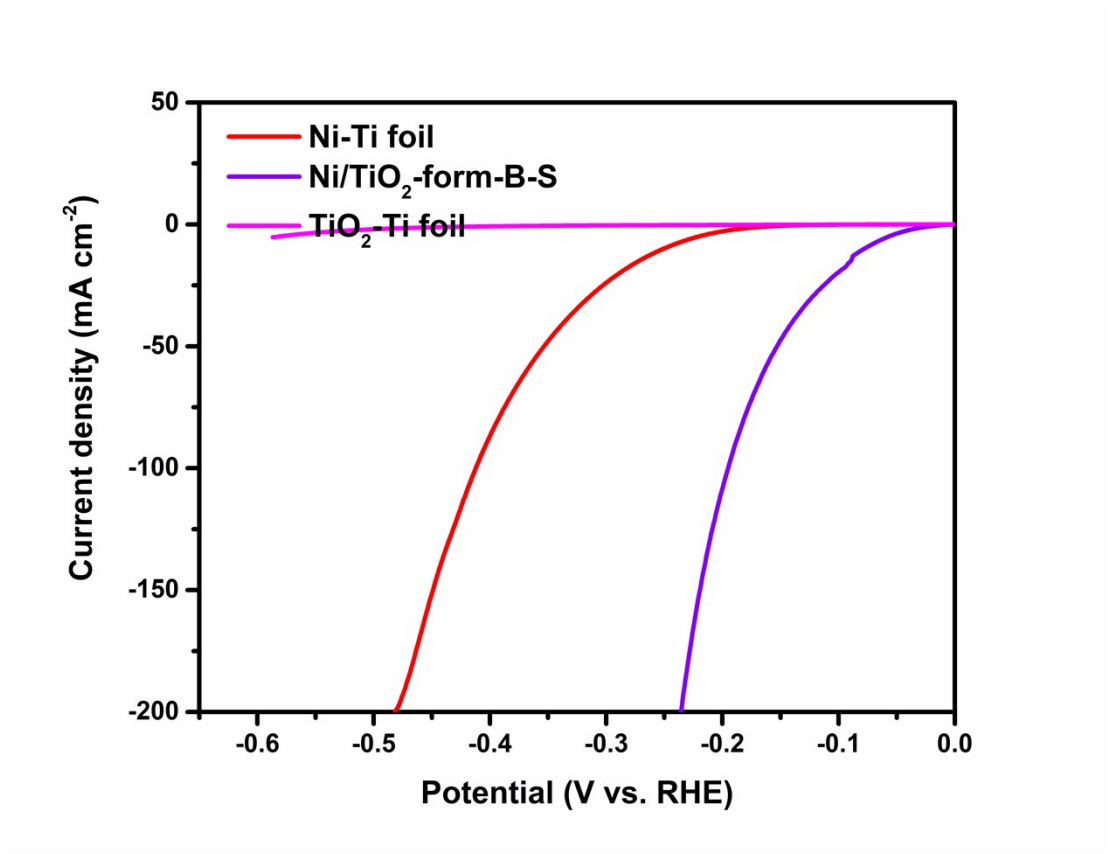

Figure S4. The LSV curves of Ni-Ti foil, Ni/TiO_2-form-B-S and TiO_2-Ti foil samples.

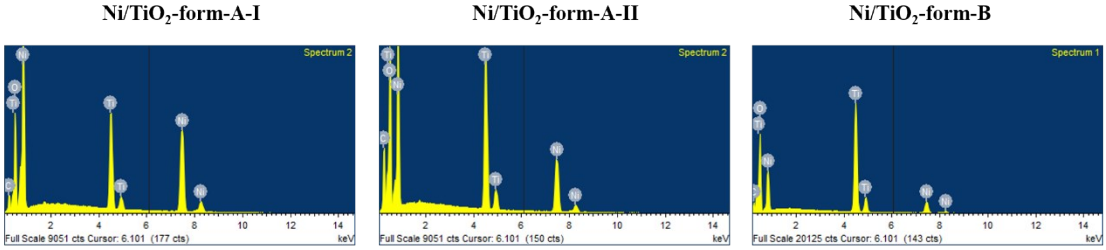

Element	Weight%	Atomic%	Element	Weight%	Atomic%	Element	Weight%	Atomic%
C K	6.13	16.91	C K	13.78	27.13	C K	4.37	8.98
O K	18.58	38.44	O K	33.57	49.62	O K	42.02	64.88
Ti K	17.27	11.93	Ti K	22.32	11.02	Ti K	37.74	19.46
Ni K	58.02	32.72	Ni K	30.33	12.23	Ni K	15.87	6.68
Totals	100.00	100.00	Totals	100.00	100.00	Totals	100.00	100.00

Figure S5. The EDS spectra of different Ni/TiO_2 samples.

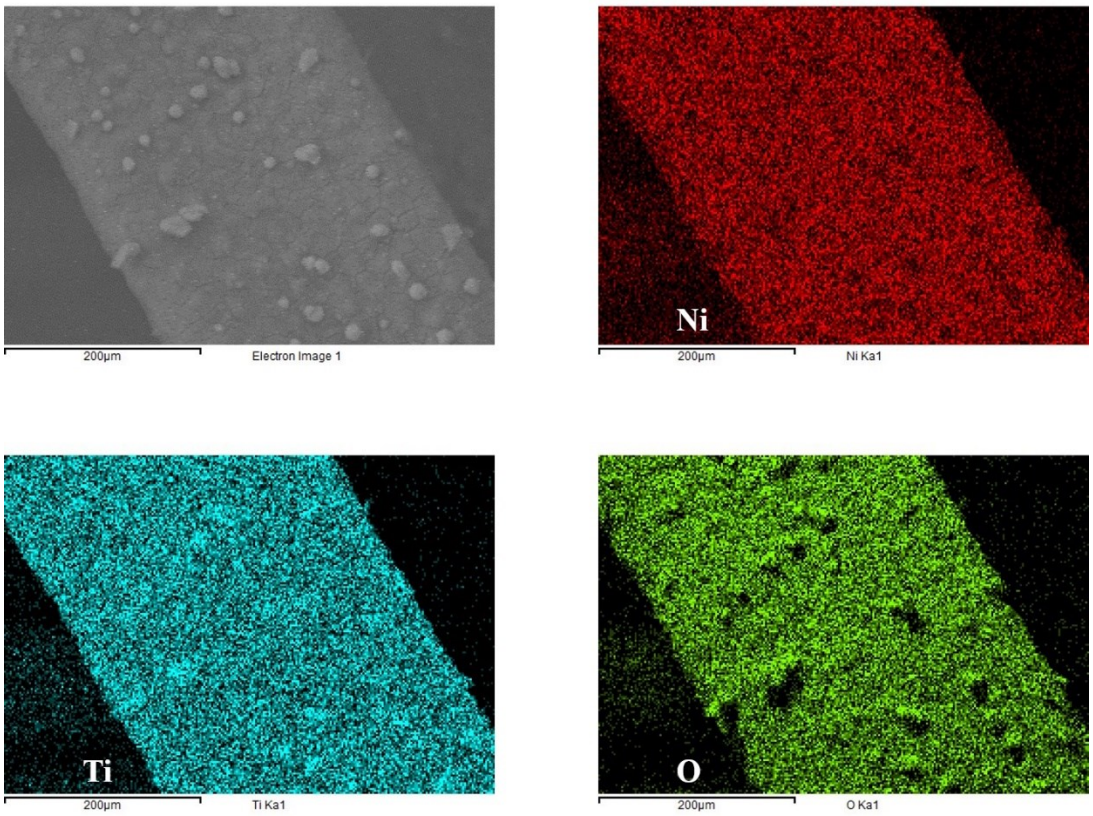

Figure S6. SEM-EDS Mapping images of Ni, Ti and O elements in Ni/TiO_2-form-A-II sample.

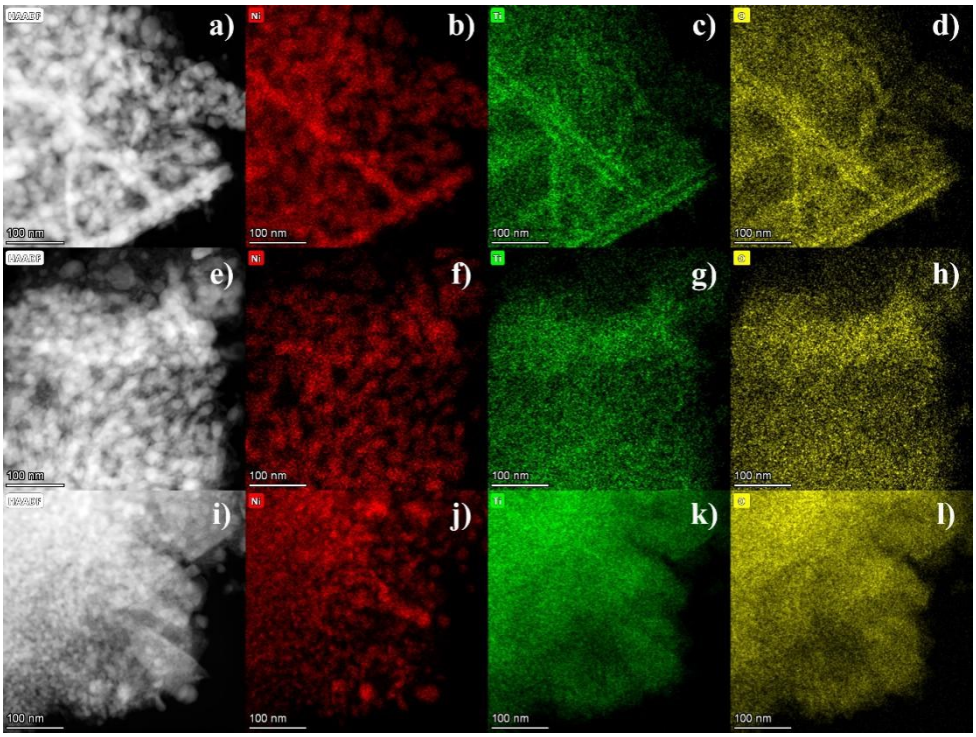

Figure S7. TEM-EDS Mapping images of Ni/TiO_2-form-A-I (a-d), Ni/TiO_2-form-A-II (e-h) and Ni/TiO_2-form-B (i-l).

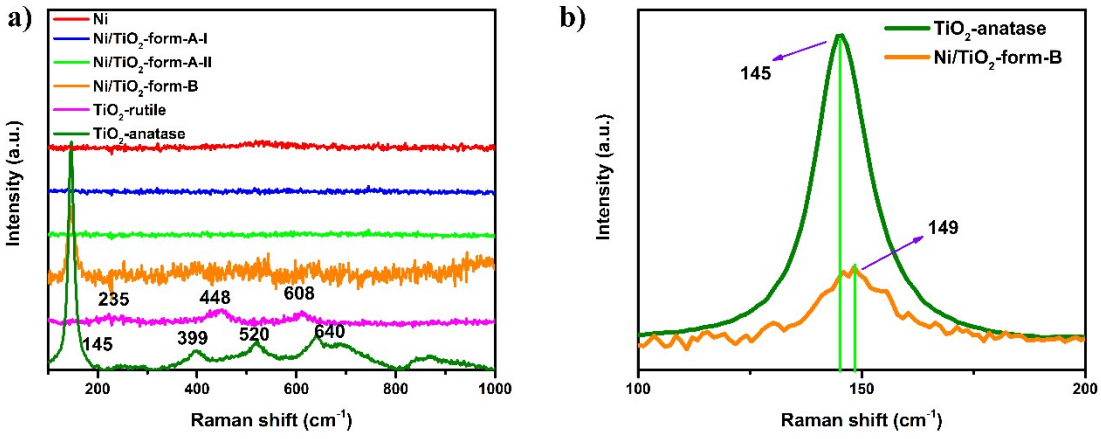

Figure S8. Raman spectra of Ni, TiO_2 with different crystal forms and Ni/TiO_2 samples with different combination forms.

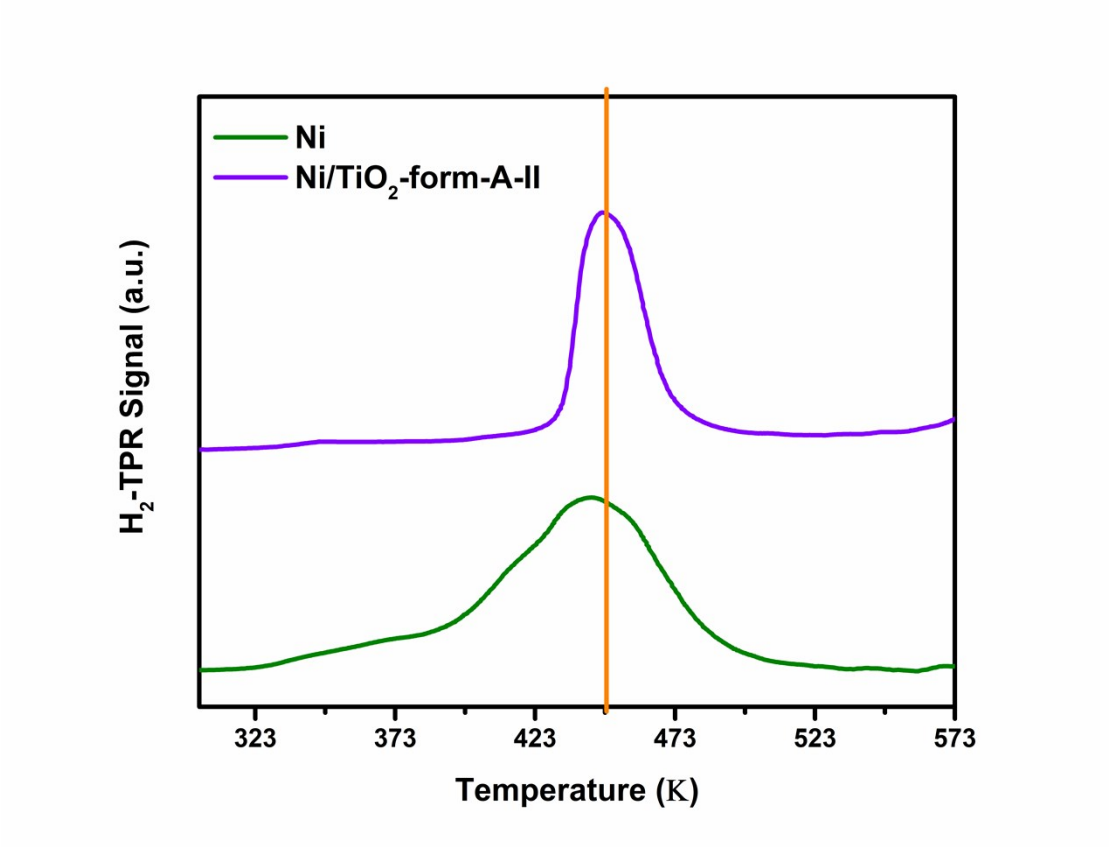

Figure S9. The H_2-TPR spectrum of Ni and Ni/TiO_2-form-A-II samples.

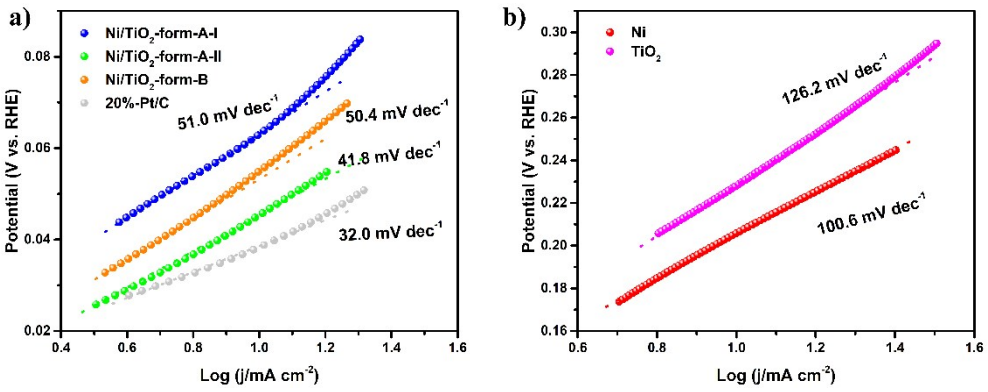

Figure S10. Tafel slope values of Pt/C, Ni, TiO_2 and Ni/TiO_2 samples with different forms in 1M KOH solution.

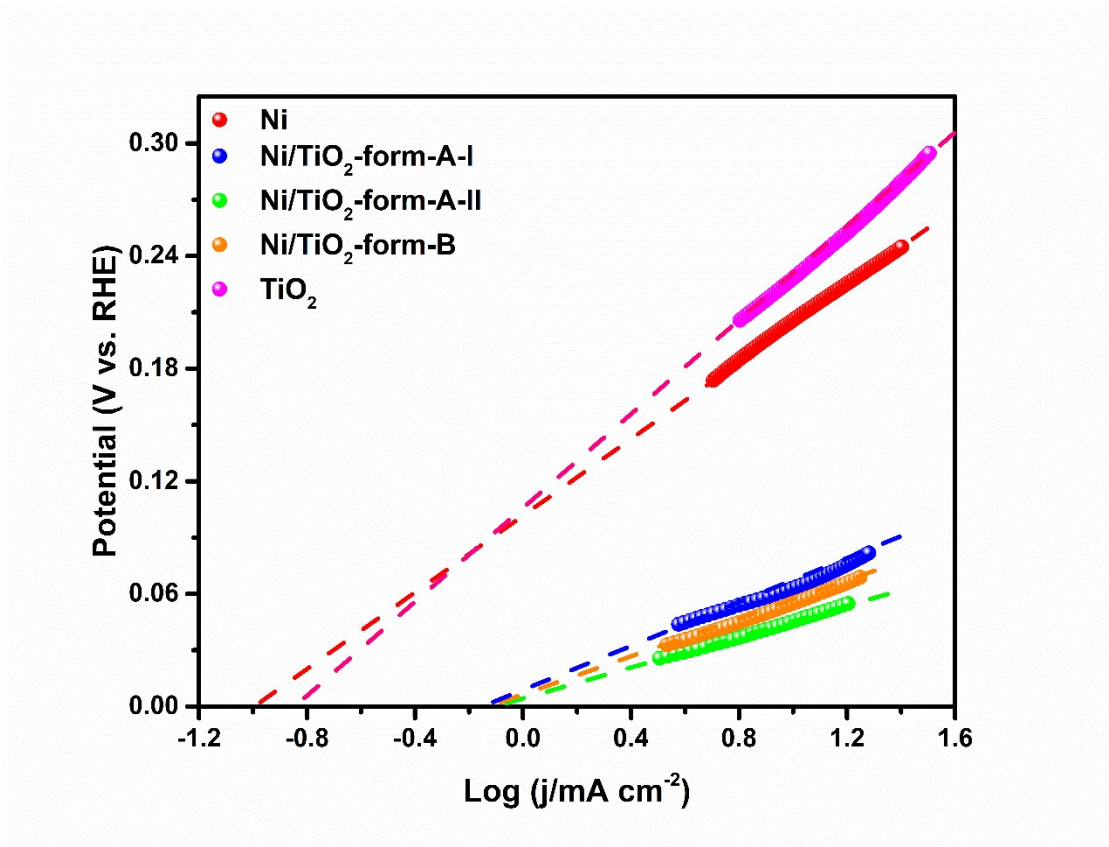

Figure S11. The exchange current density spectrum of Ni, different Ni/TiO_2 and TiO_2 samples derived from Tafel curves.

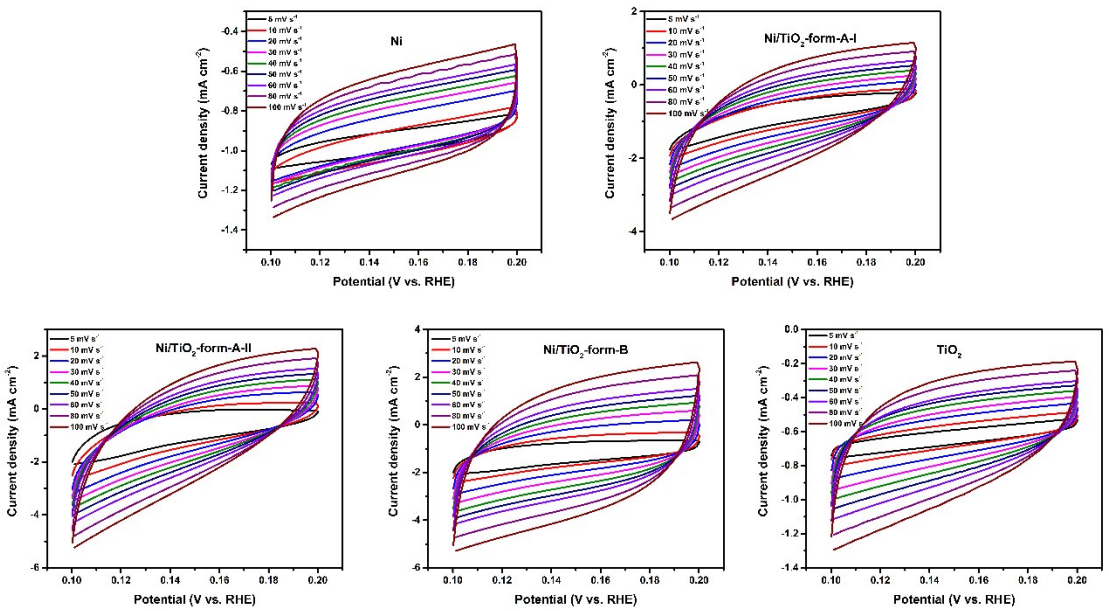

Figure S12. The electrical double-layer capacitance curves (which is proportion to electrochemical surface area (ECSA), vs. RHE) of Ni, different Ni/TiO_2 and TiO_2 samples.

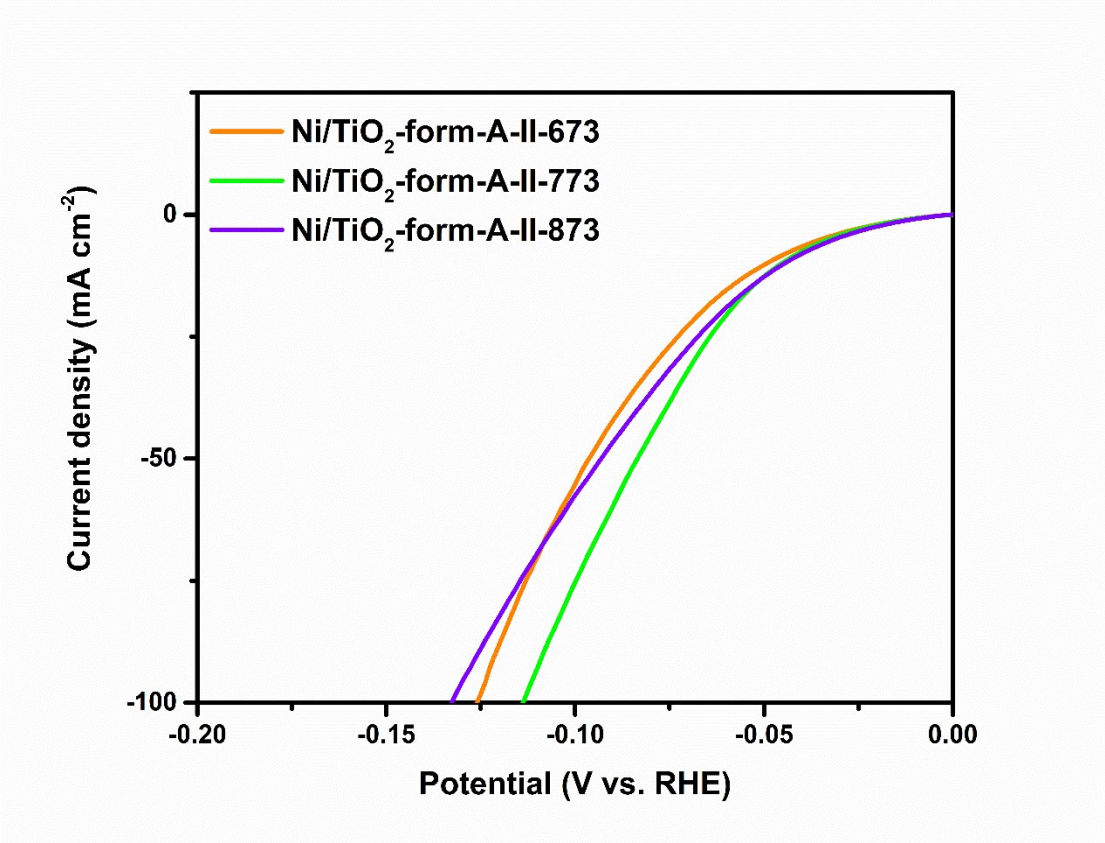

Figure S13. The LSV curves of Ni/TiO_2-form-A-II samples with different synthesized temperatures.

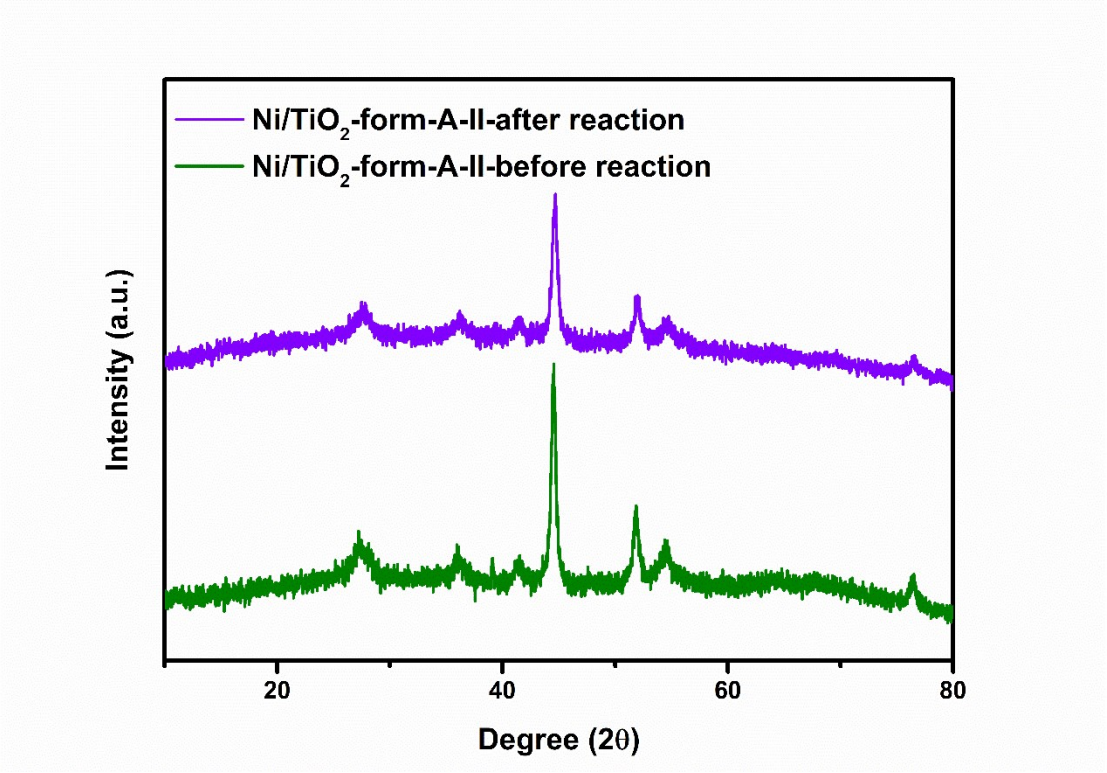

Figure S14. The XRD spectra of Ni/TiO_2-form-A-II samples before and after reaction.

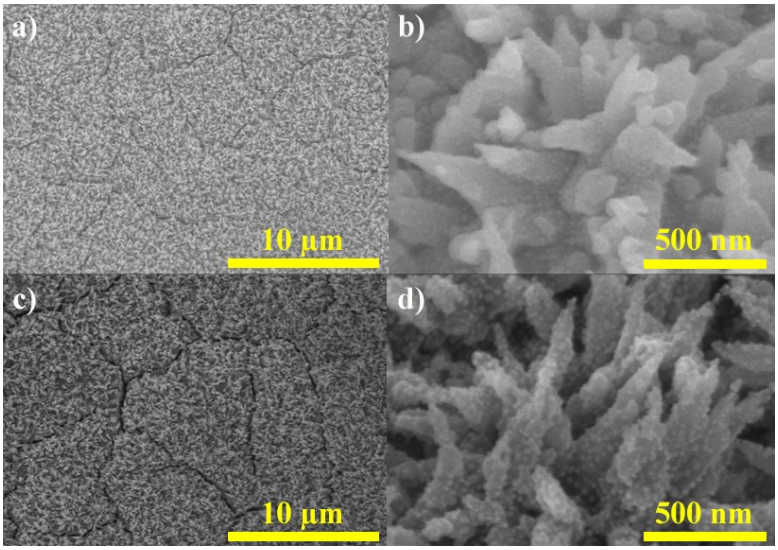

Figure S15. The SEM images of Ni/TiO_2-form-A-II samples before and after reaction.

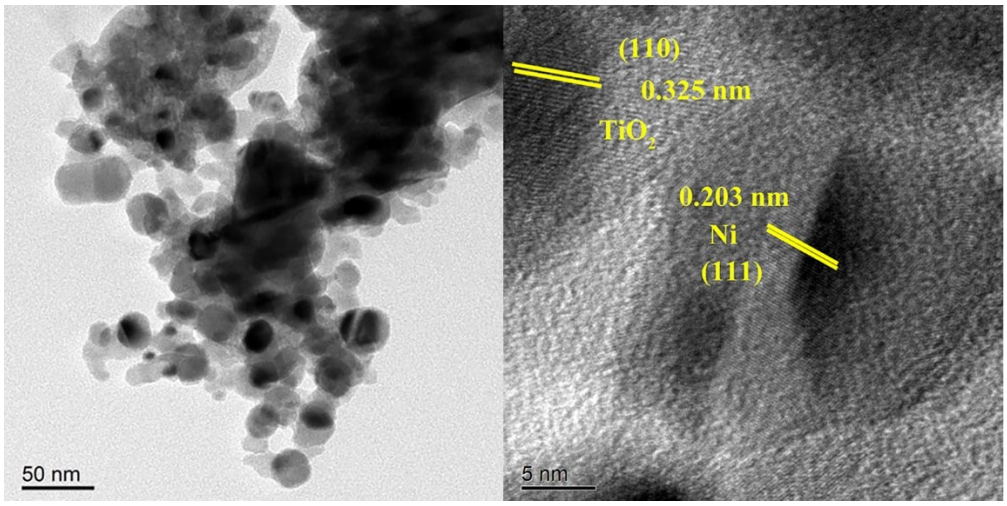

Figure S16. The TEM and HRTEM images of Ni/TiO_2-form-A-II sample after reaction.

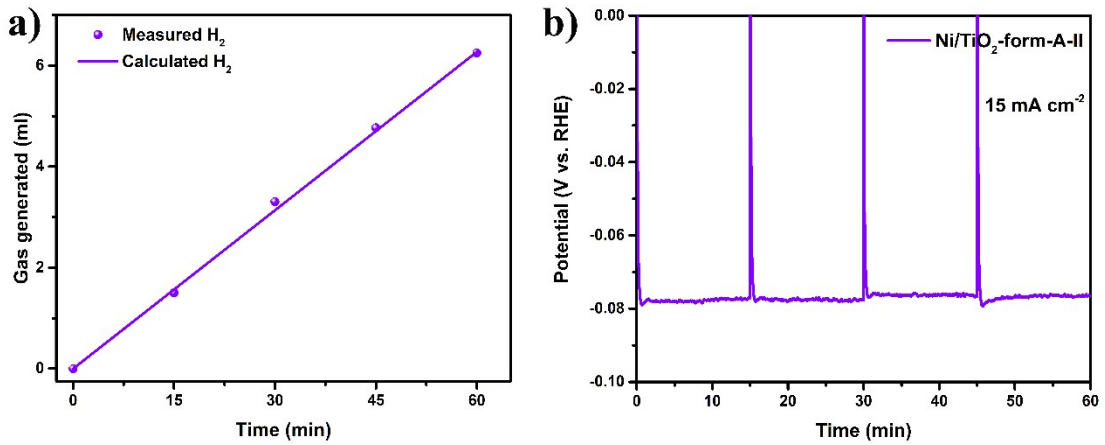

Figure S17. The amount of H_2 generated during the reaction of Ni/TiO_2-form-A-II sample and the potential-time curve (without iR correction) at the current density of 15 mA cm^{-2} over a sampling period of 1 hour.

Table S1. The performance comparison of Ni/TiO_2-form-A-II electrode with other HER materials

Catalyst	Overpotential at 10 mA cm^{-2} (mV)	Tafel slope (mV dec^{-1})	Electrolyte	Source
Ni/TiO_2-form-A-II	46	41.8	1M KOH	This work
Mo_2C-MoOx	60	53	1M $HClO_4$	[1]
NiMoOP	91	55.9	1M KOH	[2]
Co-NC	157	109	1M KOH	[3]
Ni-NiO-CNT	≈90	82	1M KOH	[4]
Co-Co_3O_4	90	90	1M KOH	[5]
Ni-V_2O_3	61	79.7	1M KOH	[6]
N-CoP_2	38	46	0.5M H_2SO_4	[7]
Ni-VC	138	62	0.5M H_2SO_4	[8]
CoP	122	54.8	0.5M H_2SO_4	[9]
MOF derived Ni	61	71	1M KOH	[10]
Ni_3N-C	115	52.1	1M KOH	[11]
Ni_2P-NiP_2	59.7	58.8	1M KOH	[12]
MoS_2-$CoNi_2S_4$	78	67	1M KOH	[13]
Al-CoS_2	86	62.47	0.5M H_2SO_4	[14]
Ni-C	37	42	1M KOH	[15]
Co-NiS_2	80	43	1M KOH	[16]

Table S2. Comparison of HER performance between our sample and the non-precious metal Ni materials reported in literatures in alkaline solution

Catalyst	η_{10}(mV)	Tafel slope (mV decade^{-1})	Electrolyte	Source
Ni/TiO_2-form-A-II	46	41.8	1 M KOH	This work
Ni@CeO_2	91	51	1 M KOH	[17]
Ni/NiO/CNT	80	82	1 M KOH	[4]
Ni-Mo	92	76	1 M KOH	[18]
Ni@C	37	57	1 M KOH	[15]
Ni@NiO	79	119	1 M KOH	[19]
Ni@$Ni(OH)_2$	68	97	1 M KOH	[20]
Ni/V_2O_3	61	79.7	1 M KOH	[6]
Ni@MoS_2	98	75	1 M KOH	[21]
Ni@Mo_2C	179	101	1 M KOH	[22]
Ni-$Ni(OH)_2$	57	44.8	1 M KOH	[23]
NiCu	184	84	1 M KOH	[24]
Ni-NiMoN	37	51	1 M KOH	[25]
NiW-W	59	52	1 M KOH	[26]
Ni-Ni_3C	98	88.5	1 M KOH	[27]
Ni-Fe_3C	93	97	1 M KOH	[28]
NiCo	72	57	1 M KOH	[29]

References

[1] L. He, W. Zhang, Q. Mo, W. Huang, L. Yang, Q. Gao, Molybdenum Carbide-Oxide Heterostructures: In Situ Surface Reconfiguration toward Efficient Electrocatalytic Hydrogen Evolution, Angew. Chem. Int. Ed, 59 (2020) 3544-3548.

[2] J. Balamurugan, T.T. Nguyen, V. Aravindan, N.H. Kim, J.H. Lee, Highly reversible water splitting cell building from hierarchical 3D nickel manganese oxyphosphide nanosheets, Nano Energy, 69 (2020) 104432.

[3] H. Huang, S. Zhou, C. Yu, H. Huang, J. Zhao, L. Dai, J. Qiu, Rapid and energy-efficient microwave pyrolysis for high-yield production of highly-active bifunctional electrocatalysts for water splitting, Energy Environ. Sci, 13 (2020) 545-553.

[4] M. Gong, W. Zhou, M.-C. Tsai, J. Zhou, M. Guan, M.-C. Lin, B. Zhang, Y. Hu, D.-Y. Wang, J. Yang, S.J. Pennycook, B.-J. Hwang, H. Dai, Nanoscale nickel oxide/nickel heterostructures for active hydrogen evolution electrocatalysis, Nat. Commun, 5 (2014) 4695.

[5] X. Yan, L. Tian, M. He, X. Chen, Three-Dimensional Crystalline/Amorphous Co/Co3O4 Core/Shell Nanosheets as Efficient Electrocatalysts for the Hydrogen Evolution Reaction, Nano Lett, 15 (2015) 6015-6021.

[6] M. Ming, Y. Ma, Y. Zhang, L.-B. Huang, L. Zhao, Y.-Y. Chen, X. Zhang, G. Fan, J.-S. Hu, 3D nanoporous Ni/V2O3 hybrid nanoplate assemblies for highly efficient electrochemical hydrogen evolution, J. Mater. Chem. A, 6 (2018) 21452-21457.

[7] J. Cai, Y. Song, Y. Zang, S. Niu, Y. Wu, Y. Xie, X. Zheng, Y. Liu, Y. Lin, X. Liu, G. Wang, Y. Qian, N-induced lattice contraction generally boosts the hydrogen evolution catalysis of P-rich metal phosphides, Sci Adv, 6 (2020) eaaw8113.

[8] L. Peng, J. Shen, L. Zhang, Y. Wang, R. Xiang, J. Li, L. Li, Z. Wei, Graphitized carbon-coated vanadium carbide nanoboscages modified by nickel with enhanced electrocatalytic activity for hydrogen evolution in both acid and alkaline solutions, J. Mater. Chem. A, 5 (2017) 23028-23034.

[9] L. Ji, J. Wang, X. Teng, T.J. Meyer, Z. Chen, CoP Nanoframes as Bifunctional Electrocatalysts for Efficient Overall Water Splitting, ACS Catal, 10 (2020) 412-419.

[10] T. Wang, Q. Zhou, X. Wang, J. Zheng, X. Li, MOF-derived surface modified Ni nanoparticles as an efficient catalyst for the hydrogen evolution reaction, J. Mater. Chem. A, 3 (2015) 16435-16439.

[11] T. Liu, M. Li, C. Jiao, M. Hassan, X. Bo, M. Zhou, H.-L. Wang, Design and synthesis of integrally structured Ni3N nanosheets/carbon microfibers/Ni3N nanosheets for efficient full water splitting catalysis, J. Mater. Chem. A, 5 (2017) 9377-9390.

[12] T. Liu, A. Li, C. Wang, W. Zhou, S. Liu, L. Guo, Interfacial Electron Transfer of Ni2P–NiP2 Polymorphs Inducing Enhanced Electrochemical Properties, Adv. Mater, 30 (2018) 1803590.

[13] J. Hu, C. Zhang, P. Yang, J. Xiao, T. Deng, Z. Liu, B. Huang, M.K.H. Leung, S. Yang, Kinetic-Oriented Construction of MoS2 Synergistic Interface to Boost pH-Universal Hydrogen Evolution, Adv. Funct. Mater, 30 (2020) 1908520.

[14] M. Wang, W. Zhang, F. Zhang, Z. Zhang, B. Tang, J. Li, X. Wang, Theoretical Expectation and Experimental Implementation of In Situ Al-Doped CoS2 Nanowires on Dealloying-Derived Nanoporous Intermetallic Substrate as an Efficient Electrocatalyst for Boosting Hydrogen Production, ACS Catal, 9 (2019) 1489-1502.

[15] H. Sun, Y. Lian, C. Yang, L. Xiong, P. Qi, Q. Mu, X. Zhao, J. Guo, Z. Deng, Y. Peng, A hierarchical nickel–carbon structure templated by metal–organic frameworks for efficient overall water splitting, Energy Environ. Sci, 11 (2018) 2363-2371.

[16] J. Yin, J. Jin, H. Zhang, M. Lu, Y. Peng, B. Huang, P. Xi, C.-H. Yan, Atomic Arrangement in Metal-Doped NiS2 Boosts the Hydrogen Evolution Reaction in Alkaline Media, Angew. Chem. Int. Ed, 58 (2019) 18676-18682.

[17] Z. Weng, W. Liu, L.-C. Yin, R. Fang, M. Li, E.I. Altman, Q. Fan, F. Li, H.-M. Cheng, H. Wang, Metal/Oxide Interface Nanostructures Generated by Surface Segregation for Electrocatalysis, Nano Lett, 15 (2015) 7704-7710.

[18] J. Tian, N. Cheng, Q. Liu, X. Sun, Y. He, A.M. Asiri, Self-supported NiMo hollow nanorod array: an efficient 3D bifunctional catalytic electrode for overall water splitting, J. Mater. Chem. A, 3 (2015) 20056-20059.

[19] J. Wang, S. Mao, Z. Liu, Z. Wei, H. Wang, Y. Chen, Y. Wang, Dominating Role of Ni0 on the Interface of Ni/NiO for Enhanced Hydrogen Evolution Reaction, ACS Appl. Mater. Interfaces, 9 (2017) 7139-7147.

[20] Z. Xing, L. Gan, J. Wang, X. Yang, Experimental and theoretical insights into sustained water splitting with an electrodeposited nanoporous nickel hydroxide@nickel film as an electrocatalyst, J. Mater. Chem. A, 5 (2017) 7744-7748.

[21] Q. Wang, Z.L. Zhao, S. Dong, D. He, M.J. Lawrence, S. Han, C. Cai, S. Xiang, P. Rodriguez, B. Xiang, Z. Wang, Y. Liang, M. Gu, Design of active nickel single-atom decorated MoS2 as a pH-universal catalyst for hydrogen evolution reaction, Nano Energy, 53 (2018) 458-467.

[22] Z.-Y. Yu, Y. Duan, M.-R. Gao, C.-C. Lang, Y.-R. Zheng, S.-H. Yu, A one-dimensional porous carbon-supported Ni/Mo2C dual catalyst for efficient water splitting, Chem. Sci, 8 (2017) 968-973.

[23] J. Hu, S. Li, Y. Li, J. Wang, Y. Du, Z. Li, X. Han, J. Sun, P. Xu, A crystalline–amorphous Ni–Ni(OH)2 core–shell catalyst for the alkaline hydrogen evolution reaction, J. Mater. Chem. A, 8 (2020) 23323-23329.

[24] M.A. Ahsan, A.R. Puente Santiago, Y. Hong, N. Zhang, M. Cano, E. Rodriguez-Castellon, L. Echegoyen, S.T. Sreenivasan, J.C. Noveron, Tuning of Trifunctional NiCu Bimetallic Nanoparticles Confined in a Porous Carbon Network with Surface Composition and Local Structural Distortions for the Electrocatalytic Oxygen Reduction, Oxygen and Hydrogen Evolution Reactions, J. Am. Chem. Soc, 142 (2020) 14688-14701.

[25] L. Shang, Y. Zhao, X.-Y. Kong, R. Shi, G.I.N. Waterhouse, L. Wen, T. Zhang, Underwater superaerophobic Ni nanoparticle-decorated nickel–molybdenum nitride nanowire arrays for hydrogen evolution in neutral media, Nano Energy, 78 (2020) 105375.

[26] Y.-K. Li, G. Zhang, H. Huang, W.-T. Lu, F.-F. Cao, Z.-G. Shao, Ni17W3–W Interconnected Hybrid Prepared by Atmosphere- and Thermal-Induced Phase

Separation for Efficient Electrocatalysis of Alkaline Hydrogen Evolution, Small, 16 (2020) 2005184.

[27] P. Wang, R. Qin, P. Ji, Z. Pu, J. Zhu, C. Lin, Y. Zhao, H. Tang, W. Li, S. Mu, Synergistic Coupling of Ni Nanoparticles with Ni3C Nanosheets for Highly Efficient Overall Water Splitting, Small, 16 (2020) 2001642.

[28] C. Yang, R. Zhao, H. Xiang, J. Wu, W. Zhong, W. Li, Q. Zhang, N. Yang, X. Li, Ni-Activated Transition Metal Carbides for Efficient Hydrogen Evolution in Acidic and Alkaline Solutions, Adv. Energy Mater, 10 (2020) 2002260.

[29] X. Tan, S. Geng, Y. Ji, Q. Shao, T. Zhu, P. Wang, Y. Li, X. Huang, Closest Packing Polymorphism Interfaced Metastable Transition Metal for Efficient Hydrogen Evolution, Adv. Mater, 32 (2020) 2002857.